



## Dibenzothiophene hydrodesulfurization over synthesized MoS<sub>2</sub> catalysts

Hamdy Farag<sup>a,b,\*</sup>, Kinya Sakanishi<sup>b</sup>, Masato Kouzu<sup>b</sup>, Akimitsu Matsumura<sup>b</sup>,  
Yoshikazu Sugimoto<sup>b</sup>, Ikuo Saito<sup>b</sup>

<sup>a</sup> Chemistry Department, Faculty of Science, Mansoura University, Mansoura 35516, Egypt

<sup>b</sup> Institute for Energy Utilization, AIST, Tsukuba West, 16-1 Onogawa, Ibaraki 305-8569, Japan

Received 29 November 2002; received in revised form 2 June 2003; accepted 7 June 2003

### Abstract

Bulk MoS<sub>2</sub> catalysts were prepared starting from various Mo-precursors. The catalytic activity was investigated for hydrodesulfurization (HDS) of dibenzothiophene (DBT) with a batch sampler attached micro-autoclave reactor at 340 °C and 3 MPa H<sub>2</sub>. In general, HDS activity was found to be inversely proportional to catalysts particle size. An interesting relationship was found between the average number of MoS<sub>2</sub> stacked layer and the selectivity of HDS in which it passes through a minimum at small crystallite sizes of ca. 4 nm and then turned up with crystallite sizes larger than 5 nm irrespective of the starting catalyst precursors. Detailed kinetics is discussed.

© 2003 Elsevier B.V. All rights reserved.

**Keywords:** Hydrodesulfurization; Crystallite size; Selectivity; MoS<sub>2</sub>; Dibenzothiophene

### 1. Introduction

Catalysts based on molybdenum-sulfide are widely used in oil refineries for the hydrotreatment (hydrodesulfurization (HDS), hydrodenitrogenation (HDN) and hydrodeoxygenation (HDO) reactions) of petroleum-derived feedstocks [1–5]. In the case of the HDS, alumina supported CoMoS and NiMoS catalysts have been traditionally used. These present industrial hydrotreating catalysts have still limited activities. Thus, due to the stringent environmental legislation that set the sulfur level at <15 ppm, new catalysts with significantly improved catalytic performance must be developed. There are a quite large

number of publications focusing on the structures and activities of supported MoCoS and/or MoNiS catalysts [6–16]. Nevertheless, only a limited number of studies have made investigations of the bulk properties of such transition metal sulfides catalysts and their effects on the activity [17–24].

It is certain that the breakthrough in developing highly active HDS catalysts is based on the accurate determination of the active sites involved in the process. There is a debate about relating the catalytic activity of HDS over molybdenum-sulfide like crystal structures to the edges and/or basal planes [11,19,20]. It is not clear if promoters like cobalt or nickel decorate the crystal structure of molybdenum-sulfides. However, some studies presumed the activity of molybdenum-sulfide to be localized at the edges and not on the flat basal planes [20]. Based on this hypothesis, MoS<sub>2</sub> with at least two stacking layers is likely

\* Corresponding author. Tel.: +81-298-61-8437;

fax: +81-298-61-8408.

E-mail address: [hamdy-farag@aist.go.jp](mailto:hamdy-farag@aist.go.jp) (H. Farag).

to be a crucial structure. This raises an essential question of the effect of crystallinity factor, i.e. mainly the number of stacking, on the catalytic activities of HDS. Basically, the HDS reaction occurs through two parallel pathways, one by direct S-extrusion and the other by hydrogenation and the catalyst modifications are supposed to control one route over the other. The role of the stacked MoS<sub>2</sub> layers in the HDS of DBT is not yet completely understood. Consequently, the nanoscale structure of molybdenum-sulfides gains more interest. An attempt to clarify the role of crystallinity, more precisely the stacked layer, of MoS<sub>2</sub> obtained from various molybdenum precursors on the network of HDS reaction is demonstrated.

## 2. Experimental section

### 2.1. Materials

Commercially available ammonium tetrathiomolybdate [(NH<sub>4</sub>)<sub>2</sub>MoS<sub>4</sub>], molybdenum(IV) acetylacetonate, ammonium heptamolybdate [(NH<sub>4</sub>)<sub>6</sub>Mo<sub>7</sub>O<sub>24</sub>·4H<sub>2</sub>O] were used as initial precursors for obtaining MoS<sub>2</sub> catalysts. Decane solvent, DBT and other chemicals are of high purity laboratory grade supplied from Wako Chemical Company.

### 2.2. Catalysts synthesis

Three series of molybdenum-sulfide phase structures (MoS<sub>2</sub>), AC, AM and TH were prepared by thermally decomposing, molybdenum(IV) acetylacetonate, ammonium heptamolybdate and ammonium thiomolybdate precursors under various experimental conditions, respectively. In a typical procedure a certain amount of the precursor powder (2.0–3.0 g) was placed in a cylindrical silica glass boat reactor and treated with a continuous flow of 10 vol.% H<sub>2</sub>S–H<sub>2</sub> gas mixture with a rate of 60 SCCM; temperature was raised at a rate of 10 °C min<sup>-1</sup>. The reaction products were trapped in a concentrated NaOH solution. The sulfidation process was kept running until the end of the theoretically estimated time for complete sulfidation and continued under the same conditions for further 1 h. Thereafter, a flow of the sulfiding gas was replaced and changed to helium with a flow rate of 50 SCCM for 30 min. Then, the system was cooled down

to the ambient temperature while keep flowing of the helium gas. This step helps purge the excess amount of H<sub>2</sub>S that is likely adsorbed on the catalyst surface. A variety of temperature condition was studied ranging from 400 to 800 °C to modify the size of the particles. Elemental analysis of the obtained catalysts powders indicates a stoichiometric molybdenum-sulfide (S/Mo atomic ratio of 2.0). The catalysts were kept in a desiccator for further examination. TH-400 is an example referring to catalyst TH and the temperature at which sulfidation was conducted.

### 2.3. Grinding

Grinding of sulfided catalysts was fulfilled using the Media Agitating Mill with helium purging for 24 h. The end letter G, accompanying the catalyst code name, refers to these treated catalysts, e.g. THG-400.

### 2.4. Surface area measurements

The BET-surface areas were measured using an automatic sorptomatic apparatus (Quantachrome) at liquid nitrogen temperature. Activation treatments were carried out at 300 °C.

### 2.5. Activity measurements

A magnetically stirred and sampler attached 100 ml micro-autoclave reactor designed to follow up the catalytic activities at various conversion levels was used. The sampling system was equipped with a 3 μm stainless steel filter to prevent suction of catalyst from the system. This special reactor design allows withdrawing an aliquot size of about 0.10 ml out from the reaction zone for analysis at frequent time intervals. This small liquid samples does not significantly decrease the amount of the feed. DBT, a common refractory sulfur compound in the crude oil, was chosen as a representative substrate for HDS reaction. The reaction was typically carried out as follows. The reactor was first charged with 100–200 mg catalysts, 500 mg copper powder and 0.5435 mM DBT in decane solvent. Then, it was flushed with hydrogen three times followed by adjusting the hydrogen pressure to 3 MPa at room temperature. The reactor was heated to 340 °C during a time of ca. 20 min.

It is worthwhile to mention that addition of copper powder helps masking the continuous self-produced  $\text{H}_2\text{S}$  during the reaction through the formation of the  $\text{CuS}$  phase. This masking significantly mitigates the kinetic interference that presumably occurred due to the inhibition by such species as discussed in a previous publication [25].  $\text{H}_2\text{S}$  was found to affect the hydrogenation and direct desulfurization reaction routes but unequally. The feed and the reaction products were monitored by a HP 6890 gas chromatograph (GC) equipped with a FID detector and with the mass spectra detector, HP5970 GC–MS, using a methylsiloxane capillary column of HP (0.32 mm  $\times$  50 m).

### 2.6. Kinetic analysis

The computer simulation empirical model that sets boundaries for the consecutive hydrodesulfurization reaction to limit the theoretical fitting errors was applied [26,27]. First order reaction scheme was assumed for all the consecutive reaction steps.

### 2.7. X-ray diffraction analysis

Catalysts were run for X-ray powder diffraction analysis on a Rigaku Geiger flex diffractometer using  $\text{Cu K}\alpha$  radiation ( $\lambda = 1.542 \text{ \AA}$ ). The following Debye–Scherrer equations were applied to estimate the average crystallite grain size of the synthesized  $\text{MoS}_2$  catalysts:

$$R_{\text{Basal}} = \frac{2\lambda}{\beta \cos 16.5^\circ} \quad (1)$$

$$R_{\text{Stack}} = \frac{0.9\lambda}{\beta \cos 7.15^\circ} \quad (2)$$

Where  $R_{\text{Basal}}$  and  $R_{\text{Stack}}$  are the average crystallite sizes of  $\text{MoS}_2$  for the basal plane (the slab length) and the plane perpendicular to the plane of the layer (the stacked layer), respectively, and  $\beta$  is the measured width at half-maximum converted to radians and  $\lambda = 1.542 \text{ \AA}$ . The appropriate shape factors for Miller indices dimensional lines of  $\text{MoS}_2$  structure (002) and (100; 101) were set as 0.9 and 2, respectively [28]. It is to be mentioned that the average crystallite sizes in the basal plane (slab length) of  $\text{MoS}_2$  were determined from broadening of the

overlap reflections due to the planes of (100) and (101).

## 3. Results

### 3.1. Catalytic activity

The catalysts have been investigated for HDS of DBT parent molecule at  $340^\circ\text{C}$  under hydrogen pressure of 3 MPa. The reaction time was extended to enable almost a full survey of the conversion level for better kinetic analysis. The main products detected in such experiments are biphenyl, phenylcyclohexane and hydrogenated dibenzothiophene in consistence with what was reported in literature [8,9,20–22]. However, a trace amount of bicyclohexane and some hydrocracked fractions are found and identified by the GC–MS. The later species are probably suspected to be obtained through the hydrocracking of phenylcyclohexane. In addition, benzene, cyclohexane and its alkylated derivatives are expected results in this reaction. However, quantifying and identifying these species at present is impossible due to the interference of their retention time with that for decane solvent. The reaction scheme can be suggested as illustrated in Fig. 1.

HDS reactions of DBT over the present catalysts were found to follow the pseudo-first order reaction mechanism. The amount of hydrogen in the reaction vessel exceeds several times as much as the required amount for full HDS. Therefore, we neglect the dependency of the reaction kinetics on hydrogen pressure. Example of typical integrated pseudo-first order reaction over the TH-400 and THG-400 catalysts are depicted in Fig. 2. The kinetic parameters extracted from the optimum fitting process for the present catalysts series are listed in Table 1. The simulation was conducted by considering the hydrocracked species to be exclusively produced from phenylcyclohexane. The hydrogenation of the partially hydrogenated DBT species is thermodynamically limited. Nevertheless, the ultimate contribution of this reaction route is possibly improved due to the fast rate of the subsequent hydrogenation reaction that eventually leads to phenylcyclohexane, i.e.  $k_{\text{D1}}$ .

One can see that, in general, the grinding results in higher activity than the unground one (Fig. 3). This

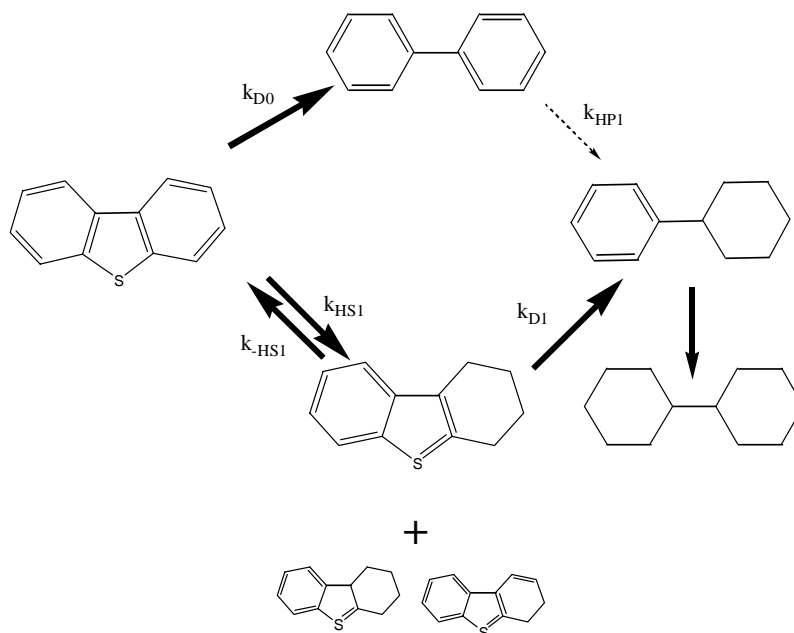


Fig. 1. Hydrodesulfurization reaction scheme of dibenzothiophene (340 °C and 3 MPa H<sub>2</sub>).

behavior is dominant regardless of various starting precursors. In addition, the partially hydrogenated DBT shows a magnitude higher reactivity than its parent DBT, very probably due to the geometric unsymmetry of this intermediate that facilitate the interaction with the catalytic active sites. However, the selectivity trends are different.

### 3.2. Selectivity of DBT-HDS over catalysts

Figs. 4 and 5 show the theoretical selectivity curves for the HDS of DBT and the experimental points obtained with AM-800 and AMG-800 catalysts. As shown in these figures, biphenyl and phenylcyclohexane are the major HDS products of DBT. However, large variations in the selectivities of the reaction are observed as can be seen from the individual

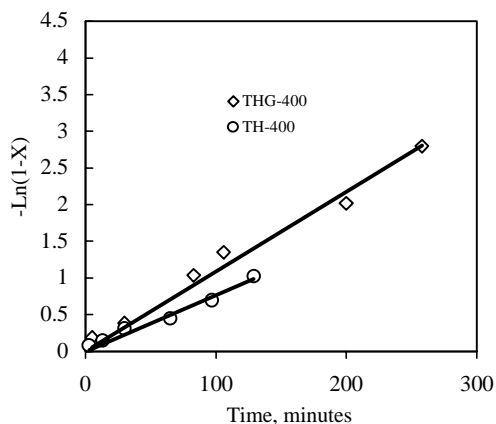


Fig. 2. Pseudo-first order kinetics of DBT-HDS over TH-400 and THG-400 catalysts (340 °C and 3 MPa H<sub>2</sub>); X: fraction converted.

Table 1  
Individual rate constants of DBT-HDS steps over bulk MoS<sub>2</sub> catalysts at 340 °C and 3 MPa H<sub>2</sub>, 10<sup>-4</sup> (g cat s)<sup>-1</sup>

Catalyst	$k_{D0}$	$k_{HS1}$	$k_{D1}$	$k_{HP1}$	$k_{-HS1}$
AC-400	1.0	0.4	31.2	<0.1	3.1
ACG-400	7.4	3.8	224.0	0.20	7.5
AC-800	2.8	1.9	8.2	<0.1	0.8
AM-800	0.4	0.1	7.9	<0.1	0.4
AMG-800	10.3	13.5	259.0	0.1	10.4
TH-400	3.7	4.5	93.6	0.1	3.7
THG-400	7.2	4.7	145.2	<0.1	7.3
TH-500	3.1	4.0	17.4	<0.1	0.7
TH-600	0.9	0.7	17.3	<0.1	0.9
TH-700	0.8	0.5	15	<0.1	0.7
TH-800	0.6	0.2	28.6	0.1	1.1

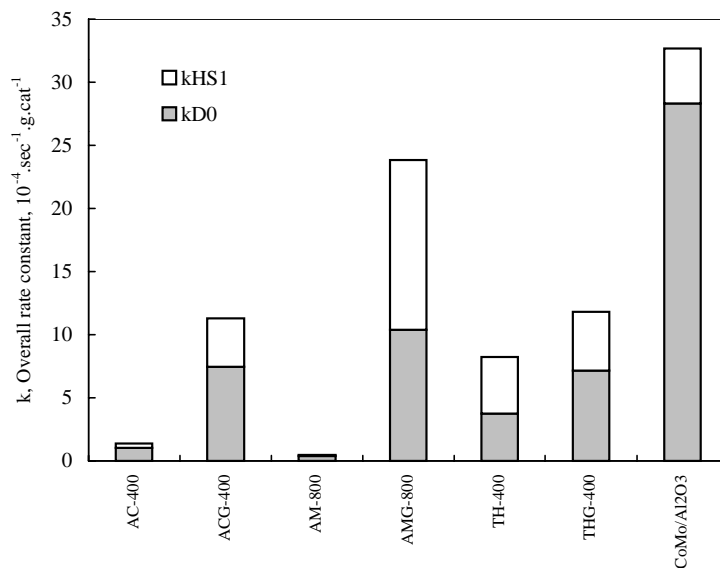


Fig. 3. DBT-HDS activity over MoS<sub>2</sub> catalysts (340 °C and 3 MPa H<sub>2</sub>).

rate constants of the reaction scheme summarized in Table 1.

While the grinding process did enhance the catalytic activity towards HDS of DBT as a general behavior, the enhancement for the two reaction pathways,  $k_{D0}$  and  $k_{HS1}$ , occurs to a somewhat different extent depending on the catalyst identity.

### 3.3. Effect of temperature and grinding on the crystallinity of catalysts

The results of the estimated average crystallite grain size and consequently the number of the stacked MoS<sub>2</sub> layers, MoS<sub>2</sub> layer thickness of 6.15 Å, for the present catalysts are described in Table 2. The variations of

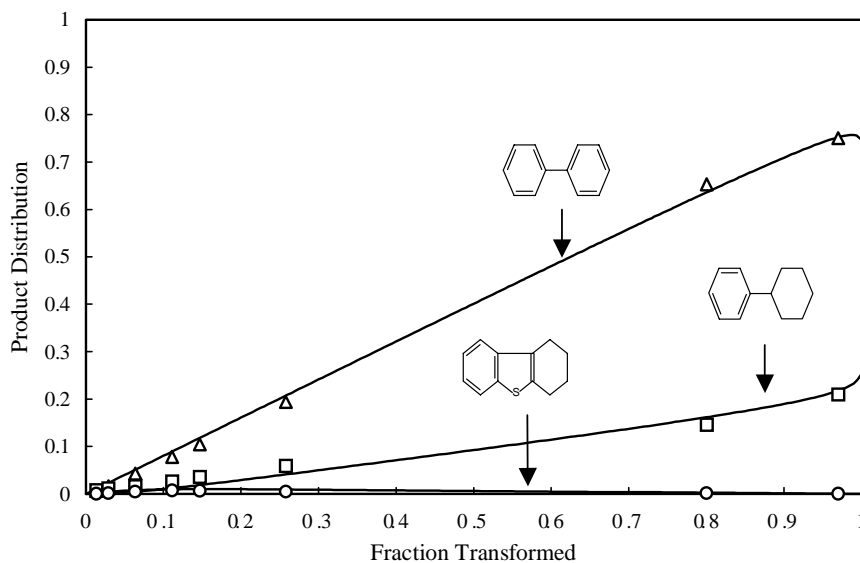


Fig. 4. Selectivity curves of DBT-HDS over AM-800 (340 °C and 3 MPa H<sub>2</sub>).

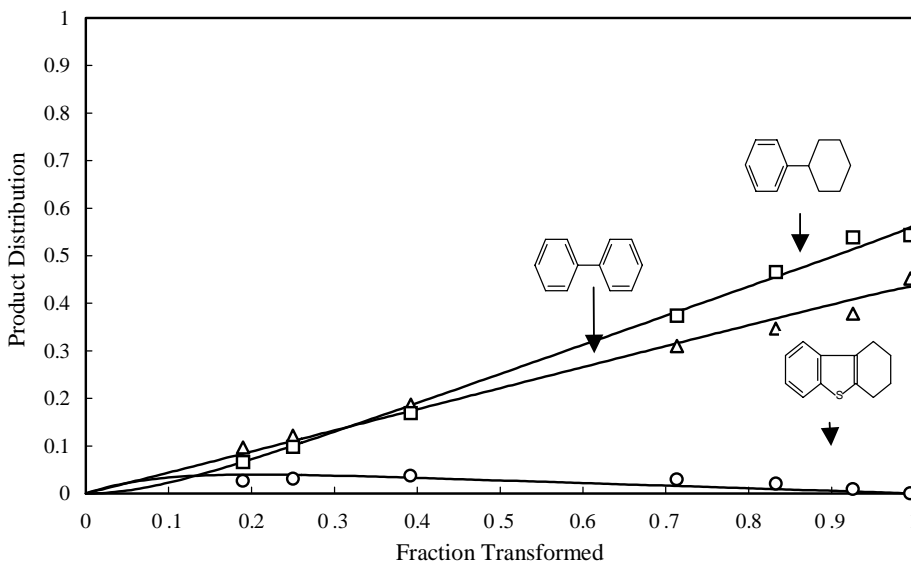


Fig. 5. Selectivity curves of DBT-HDS over AMG-800 (340°C and 3 MPa H<sub>2</sub>).

the particle size along the basal plane (the slab length) for the present catalysts series are quite small. Thus, its role in activity could be neglected. However, the development in the crystallinity, more precisely the stacked MoS<sub>2</sub> layers, is dependent on the temperature of treatments and grinding. Generally and irrespective of the catalysts origin, as the sulfidation temperature increased the number of the stacked MoS<sub>2</sub> layers gradually increased. The grinding, however, shows

another distinguished feature. Grinding of the highly crystalline MoS<sub>2</sub> catalyst, i.e. AM-800, leads to a crystallite size of about four times smaller than the initial, i.e. AMG-800. On the other hand, interestingly, grinding of the TH-400 catalyst that already consists of fine grain particles, ~4 nm, leads to larger size indicating the possibility of reconstruction of the MoS<sub>2</sub> layers. This could probably be explained in view of the particles agglomeration phenomena. It is well known that

Table 2

Apparent average crystallite sizes and BET surface areas of various synthesized MoS<sub>2</sub> catalysts

Catalyst	BET-surface area (m <sup>2</sup> g <sup>-1</sup> )	Average crystallite size <sup>a</sup> , in the (002) plane		Average crystallite size (nm), in the basal plane
		Size (nm)	No. of layers	
AC-400	<1	ND <sup>b</sup>	1–2	ND
ACG-400	14	2.4	4	4.6
AC-800	<1	2.9	5	5.4
AM-800	13	18.6	30	5.0
AMG-800	118	4.1	7	4.6
TH-400	65	3.8	6	4.5
THG-400	105	8	13	4.5
TH-500	–	4.7	8	4.7
TH-600	–	6.6	11	4.8
TH-700	–	13.4	22	4.8
TH-800	<1	20	33	5.3

<sup>a</sup> Estimated from Scherrer equation.

<sup>b</sup> Not determined.

an energy of as low as Van der Waals forces holds the layers of MoS<sub>2</sub> stacking structure [21]. This unique property of MoS<sub>2</sub> like-structure is well known and being used as lubricants and for intercalation as well. The agglomeration trend can also be noticed for ACG-400.

## 4. Discussion

### 4.1. HDS activity

Table 1 reports the estimated individual rate constants in the previous suggested reaction scheme for the studied catalysts. To a first approximation, as the number of stacked MoS<sub>2</sub> layers increased the overall HDS apparent activity decreased. However, grinding of some catalysts significantly influences the ratio of product composition (selectivity), activity, surface area and crystallite sizes. Ground catalyst series show high activity for HDS than the corresponding unground ones. The difference in the magnitude of the surface area variation with grinding is worthy noting (Table 2). The observed increase in the measured surface area of ground catalysts is probably due to the aggregates formation of the particles that leads to some porosity. Texture and morphology of these samples seem to be an essential factor that needs further study.

Direct correlation between catalytic activity and BET surface area of some catalysts could be observed in Fig. 6. However, the degree of the HDS activity enhancement against the surface area is dependent on the individual starting catalyst precursors. Anyway, grinding seems to be an effective alternate that can be used to modify the structural properties of the MoS<sub>2</sub> catalysts.

### 4.2. Catalytic selectivity of DBT-HDS

Consideration of alternative reaction pathways for HDS of the polyaromatic sulfur compounds in order of increasing difficulty based on the well known steric hindrance caused by the alkyl-substituents may be a fruitful way of searching for an appropriate catalyst. The studied catalysts exhibited a variety of the selectivity, defined as the ratio of  $k_{D0}/k_{HS1}$ . The constancy of the ratio of  $k_{D0}/(k_{D0} + k_{D1})$  and/or  $k_{HS1}/(k_{HS1} + k_{HP1})$  independent of the catalysts, extracted from Table 1, reflects the existence of two distinct active sites [5]. An interesting relation was found between the crystallite size, i.e. the number of the stacked MoS<sub>2</sub> layers, and the selectivity (Fig. 7). One can notice that for the nanoscale crystallite grain size below 4 nm, the selectivity was preferred for the direct desulfurization route. Then, the ratio passes through a minimum at a size of about 4 nm and start

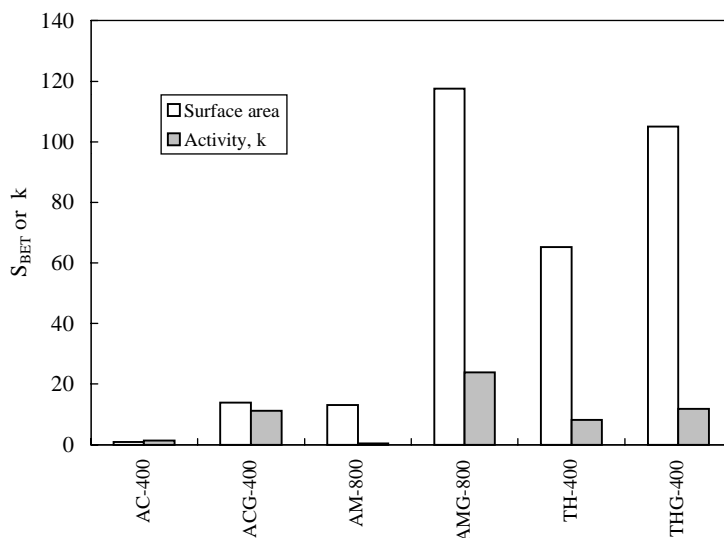


Fig. 6. Surface areas and catalytic DBT-HDS activities over various catalysts:  $S_{BET}$  (m<sup>2</sup> g<sup>-1</sup>);  $k$ , 10<sup>-4</sup> (g cat s)<sup>-1</sup>.

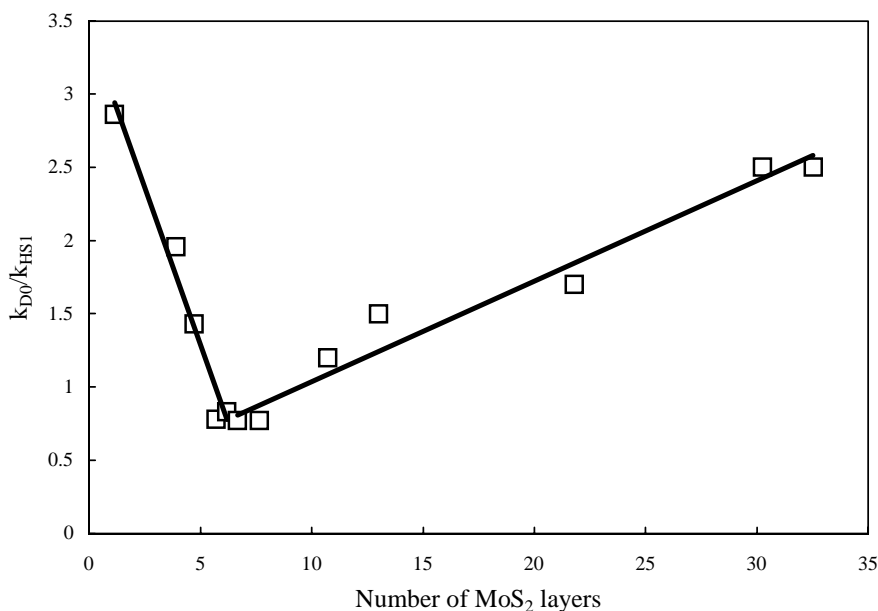


Fig. 7. Number of MoS<sub>2</sub> layers vs. selectivity in DBT-HDS.

to increase sharply again for the size larger than 5 nm. Indeed, such a trend can be extracted from literature with some shifts in the minimum value of selectivity ( $k_{D0}/k_{HS1}$ ) for HDS of both DBT and thiophene over supported CoMo catalysts [29]. This study [29] did not realize it in such way in spite of their experimental evidence. Such a relation between the selectivity and the average grain size could explain the selectivity trend for the supported catalysts. CoMo/Al<sub>2</sub>O<sub>3</sub>, for example, has a molybdenum layer that ranges between 1 and 3. It is well known that the selectivity in HDS of DBT over as-like catalysts is much more pronounced for the hydrogenolysis of C–S bond. Thus, it is not only the high stacked number of MoS<sub>2</sub> layers that show preference for direct desulfurization but also the stacked structure of mono-layers and/or a few layers behaves similarly. However, as can be seen in Fig. 7, the MoS<sub>2</sub> particles in the range of 3.5–4.7 nm, regardless the catalysts origin, exhibit a tendency for hydrogenation as the most preferred mode in HDS of DBT.

Fig. 7 can be recognized as being composed of two independent lines regarding the selectivity point of view, one is inversely proportional to the crystallite size and the other directly proportional to the crystal-

lite size. They intersect together at an inflection point (mimic of the curve). Determination of the crystallite size at this inflection point seems to be crucial as it reflects the dramatic change in the selectivity trend.

In essence, it can be proposed that the apparent effect of the crystallite grain size in the selectivity of HDS of DBT is managed by the following two equations:

$$S_1 = k_1 R_1 + M_1 \quad \text{in which } R_1 \geq 4 \text{ nm} \quad (3)$$

$$S_2 = \frac{k_2}{R_2} + M_2 \quad \text{in which } R_2 \leq 4 \text{ nm} \quad (4)$$

Where  $S_1$  and  $S_2$  are the selectivities expressed as  $k_{D0}/k_{HS1}$ ;  $R_1$  and  $R_2$  the crystallite grain sizes;  $k_1$ ,  $k_2$ ,  $M_1$  and  $M_2$  the numerical constants.

Apparently, these two straight lines intersect at a grain size of about 4 nm. So far, these equations describe the effect of grain size of MoS<sub>2</sub> catalysts on the selectivity of DBT-HDS as no inhibition is included. Inhibitors, like H<sub>2</sub>S and aromatic compounds, are regarded to have a drastic change in the selectivity in HDS of DBT. Thus, a precise control of the crystallite grain size of MoS<sub>2</sub> catalyst may provide the opportunity to adapt certain selectivity level in HDS of DBT.



The parabolic nature of the selectivity with the particle size, Fig. 7, could be explained in the light of the electronic properties of MoS<sub>2</sub>. Recently [30,31], it was reported that for MoS<sub>2</sub> when the particle size becomes comparable to or less than that of the exciton, the optical and electronic properties vary strongly with the particle size. A model parabolic relation between the charge densities and the crystallite size was found for a similar sulfide phases. This consequently may affect the geometry of adsorption of DBT on the active site whether it is flat adsorption via the delocalization of aromatic electrons or directly via the S-atom in the thiophene ring. More physical studies are encouraged for such phenomena.

In addition, our results are not consistent in some parts with the rim-edge model results [20]. In the rim-edge model, a straightforward relation between the crystallite size and selectivity was recorded which is partly in agreement with the curve in Fig. 7 for large particle size portion, i.e. Eq. (1). However, this model is difficult to interpret the high selectivity for direct desulfurization against hydrogenation for the nanoscale particles like the classic CoMo/Al<sub>2</sub>O<sub>3</sub> catalysts and some of the present catalysts as well. HDS of DBT over these catalysts was observed to proceed preferentially through the direct desulfurization route,  $k_{D0} > k_{HS1}$ . The main difference is likely attributed to the lack of data for MoS<sub>2</sub> nanostructure having mono-layers or a few stacked layers. Therefore, we can summarize the main questionable points of difference as follows:

1. In the rim-edge model, the HDS reaction of DBT were studied only for a low conversion level; it was ~60% for the highest one and for the rest catalysts in the range of 13–55%. The theoretical fitting with such a few data on the conversion level could probably lead to maximizing the erroneous factor and consequently misinterpretation of results. In our results, the conversion level was higher than 95%. In comparison, this will definitely minimize the estimated error in the numerical fitting for the rate constants determinations.
2. In the rim-edge model, it neglects the influence of H<sub>2</sub>S self-produced during reaction. It has been confirmed that H<sub>2</sub>S has a serious inhibition effect on the HDS reaction over CoMo catalysts supported on carbon and/or alumina [11,13,26] even at

the early stages of the reaction. The inhibition was clear especially for the direct desulfurization route. In the present study, H<sub>2</sub>S was almost quantitatively eliminated via its continuous scrubbing during reaction by copper powder addition. This will certainly bring down its contribution and/or interference in the reaction scheme to the lowest value.

3. In addition, recent experimental results from the same laboratory contradict with this model leading them to conclude that a simple morphological effect modifying only the relative proportion of rim sites versus edge sites is not sufficient to explain the strong change in selectivity for HDS of DBT.

Nevertheless, it appears that the crystallite grain size has a profound influence on the selectivity of HDS of DBT regardless the catalyst preparation method. It is uncertain if this behavior remains for other substrates, like 4,6-dimethyldibenzothiophene and its derivatives. More detailed study is needed and encouraged to get better understanding of these phenomena.

## 5. Conclusion

A series of bulk molybdenum-sulfide catalysts were synthesized starting from various precursors. Catalysts after grinding show higher catalytic activity for HDS of DBT than the corresponding unground one. This could be due to the creation of small grains and the increase in the active surface area of the catalysts. However, the selectivity was found to be related to the crystallite size. In reality the effect of crystallite size on the selectivity of HDS can be considered as if two straight lines intersect at certain crystallite grain size. Both very fine and large crystals may show the selectivity against direct desulfurization but small one with about 4 nm size is likely to shift the selectivity to the hydrogenation route. The HDS of DBT is suggested to occur over two distinct active sites and the selectivity is a particle size sensitive reaction (PSSR).

## Acknowledgements

This work has been entrusted by the New Energy and Industrial Technology Development Organization

under a subsidy of the Ministry of Economy, Trade and Industry.

## References

- [1] J.M. Thomas, W.J. Thomas, Principles and Practice of Heterogeneous Catalysis, VCH, New York, 1997.
- [2] B. Delmon, Y.W. Li, J. Mol. Catal. Part A: Chem. 127 (1997) 163.
- [3] B.C. Gates, Catalytic Chemistry, Wiley, New York, 1992.
- [4] D.D. Whitehurst, T. Isoda, I. Mochida, Adv. Catal. 42 (1998) 345.
- [5] B.C. Gates, J.R. Katzer, G.C.A. Schuit, Chemistry of Catalytic Processes, McGraw-Hill, New York, 1979, pp. 390–445.
- [6] P. Ratansamy, S. Sivasanker, Catal. Rev. -Sci. Eng. 22 (1980) 401.
- [7] P.T. Vasudevan, J.L.G. Fierro, Catal. Rev. -Sci. Eng. 38 (2) (1996) 161.
- [8] L. Coulier, V.H.J. de Beer, J.A.R. van Veen, J.W. Niemantsverdriet, J. Catal. 197 (2001) 26.
- [9] R. Cattaneo, T. Shido, R. Prins, J. Catal. 185 (1999) 199.
- [10] M.L. Vrinat, Appl. Catal. 6 (1983) 137.
- [11] H. Topsøe, B.S. Clausen, F.E. Massoth, Hydrotreating Catalysts, Catalysis Science and Technology, vol. 11, Springer-Verlag, New York, 1996.
- [12] A.N. Startsev, Catal. Rev. -Sci. Eng. 37 (3) (1995) 353.
- [13] K.S. Chung, F.E. Massoth, J. Catal. 64 (1980) 320.
- [14] Y. Okamoto, Catal. Today 39 (1997) 45.
- [15] C. Wivel, B. Clausen, R. Candia, S. Mørup, H. Topsøe, J. Catal. 87 (1984) 497.
- [16] F.E. Massoth, Advances in Catalysis and Related Subjects, vol. 27, Academic Press, New York, 1978, p. 265.
- [17] R.R. Chianelli, G. Berhault, Catal. Today 53 (1999) 357.
- [18] H. Topsøe, et al., J. Chem. Soc., Faraday Trans. I 83 (1987) 2157.
- [19] R.R. Chianelli, M. Daage, M.J. Ledoux, Adv. Catal. 40 (1994) 177.
- [20] M. Daage, R.R. Chianelli, J. Catal. 194 (1994) 414.
- [21] K.C. Pratt, J.V. Sanders, V. Christov, J. Catal. 124 (1990) 416.
- [22] N. Hermann, M. Brorson, H. Topsøe, Catal. Lett. 65 (2000) 169.
- [23] Y. Iwata, K. Sato, T. Yoneda, Y. Miki, Y. Sugimoto, A. Nishijima, H. Shimada, Catal. Today 45 (1998) 353.
- [24] M.M. Mdleleni, T. Hyeon, K.S. Suslick, J. Am. Chem. Soc. 120 (1998) 6189.
- [25] H. Farag, I. Mochida, K. Sakanishi, Appl. Catal. Part A: Gen. 194–195 (2000) 147.
- [26] H. Farag, D.D. Whitehurst, K. Sakanishi, I. Mochida, Catal. Today 50 (1999) 49.
- [27] D.D. Whitehurst, H. Farag, T. Nagamatsu, K. Sakanishi, I. Mochida, Catal. Today 45 (1998) 299.
- [28] H.P. Klug, L.E. Alexander, X-ray Diffraction Procedures for Polycrystalline and Amorphous Materials, second ed., Wiley, New York, 1974.
- [29] E.J.M. Hensen, P.J. Kooyman, Y. van der Meer, A.M. van der Kraan, V.H.J. de Beer, J.A.R. van Veen, R.A. van Santen, J. Catal. 199 (2001) 224.
- [30] L. Brus, J. Phys. Chem. 90 (1986) 2555.
- [31] V. Chikan, D.F. Kelley, J. Phys. Chem. 106 (2002) 3794.